

Synthesis and Evaluation of 3-Aroylindoles as Anticancer Agents: Metabolite Approach

Yu-Shan Wu,^{†,‡,§} Mohane Selvaraj Coumar,^{†,§} Jang-Yang Chang,^{§,¶} Hsu-Yi Sun,[†] Fu-Ming Kuo,[†] Ching-Chuan Kuo,[§] Ying-Jun Chen,[†] Chi-Yen Chang,[§] Chia-Ling Hsiao,[†] Jing-Ping Liou,^{||} Ching-Ping Chen,[†] Hsien-Tsung Yao,[†] Yi-Kun Chiang,[†] Uan-Kang Tan,[⊥] Chiung-Tong Chen,[†] Chang-Ying Chu,[†] Su-Ying Wu,[†] Teng-Kuang Yeh,[†] Chin-Yu Lin,[†] and Hsing-Pang Hsieh^{*,†}

[†]Division of Biotechnology and Pharmaceutical Research, National Health Research Institutes, 35 Keyan Road, Zhunan, Miaoli County 350, Taiwan, Republic of China, [‡]Department of Chemistry, Tunghai University, 181 Taichung Harbor Road Section 3, Taichung 407, Taiwan, ROC, [§]National Institute of Cancer Research, National Health Research Institutes, Tainan 704, Taiwan, ROC, ^{||}College of Pharmacy, Taipei Medical University, Taipei 110, Taiwan, ROC, and [⊥]Department of Chemical and Materials Engineering, Technology and Science Institute of Northern Taiwan, Taipei 112, Taiwan, ROC. [¶]These authors contributed equally to this work.

Received January 16, 2009

BPR0L075 (**2**) is a potential anticancer drug candidate designed from Combretastatin A-4 (**1**) based on the bioisosterism principle. Metabolites of **2**, proposed from in vitro human microsome studies, were synthesized, leading to the identification of metabolite-derived analogue **10** with 40–350 pM potency against various cancer cell lines. Insights gained from the major inactive metabolite of **2** led to the development of **29**, with better pharmacokinetics and improved potency in the tumor xenograft model than **2**.

Introduction

The high costs, long development times, and high failure rate typically associated with bringing drugs to the market have prompted drug-discovery scientists to look more critically and at an earlier stage at one of the key factors for drug candidate failure until a decade ago: drug metabolism and pharmacokinetics (PK^a).^{1,2} For example, in 1991, approximately 40% of the drug attrition rate was attributed to adverse PK issues; in 2000, however, PK issues contributed to only 10% of drug attrition.² This improvement, effected by a better understanding of the PK properties of the candidate drugs, helped to eliminate risky candidates at an early stage of drug development. In view of this, drug metabolism, one of the factors affecting the PK profile of a drug, and metabolite identification have become integral parts of early drug discovery programs.³ Drugs undergo a series of biotransformation reactions inside the body, in which more water-soluble metabolites are formed so that the body can remove these xenobiotic substances more easily. These metabolites could result in pharmacological or toxicological activity or inactivity. Although in most cases the metabolism of drugs leads to pharmacological inactivation, active metabolites have also been detected occasionally. Some of the active metabolites of marketed drugs have in fact been developed into new drugs such as acetaminophen and fexofenadine.³ The metabolism of parent compounds leading to the formation of pharmacologically active metabolites may therefore be used as an advantage during lead optimization in drug development. Also, in

cases in which inactive metabolites are formed, appropriate structural modification could decrease the drug metabolism, resulting in improved drug exposure.

Our research group has worked on the design and synthesis of antimitotic agents.^{4–6} On the basis of bioisosteric replacement of the olefinic linker and B ring in the Combretastatin A-4 (CA4, **1**) skeleton, 6-methoxy-3-(3',4',5'-trimethoxybenzoyl)-1*H*-indole (**2**, BPR0L075) was designed (Figure 1).⁵ This compound, **2**, not only exhibited potent in vitro activity against a variety of human tumor cell lines, at iv doses of 50 mg/kg, it also showed activity against xenograft tumor models of gastric carcinoma MKN-45 and human cervical carcinoma KB in nude mice.⁷ We are planning a phase I clinical trial to assess compound **2**'s potential as an anticancer agent. Recent studies using liquid chromatography tandem mass spectrometry (LC/MS/MS) on the in vitro metabolic fate of antitumor agent **2** indicated three metabolites were derived from hydroxylation on the indole moiety and that three other metabolites were derived from *O*-demethylation.^{8,9} The structural identity of five out of the six possible metabolites were confirmed unequivocally as **4–8** by comparison of the HPLC retention time and MS/MS data of the metabolites with synthetic samples.⁸ Here we report the synthesis of various possible phase I metabolites of **2** and their biological evaluation. Identification of the active metabolite of **2** led to the design and synthesis of analogue with potent in vitro cytotoxicity in the picomolar range. In addition, on the basis of the insight gained about the major metabolic elimination pathways of **2**, we have identified compound **29**, which has better in vitro and in vivo pharmacokinetic profiles and improved in vivo efficacy in the tumor xenograft model than that of parent compound **2**.

Chemistry

Possible metabolites of **2**, both demethylated and hydroxylated, are listed in Figure 1. We previously reported the

*To whom correspondence should be addressed. Phone: +886-37-246-166 ext. 35708. Fax: +886-37-586-456. E-mail, hphsieh@nhri.org.tw.

^a Abbreviations: AUC, area under curve; CA4, Combretastatin A-4; CL, clearance; iv, intravenous; H460, human lung cancer cell line; HT-29, colorectal carcinoma cell line; KB, human cervical carcinoma cell line; LCMS, liquid chromatography coupled mass spectrometry; MKN-45, gastric carcinoma cell line; NCS, *N*-chlorosuccinimide; NIS, *N*-iodosuccinimide; PK, pharmacokinetics; SAR, structure–activity relationship; *t*_{1/2}, plasma half-life.

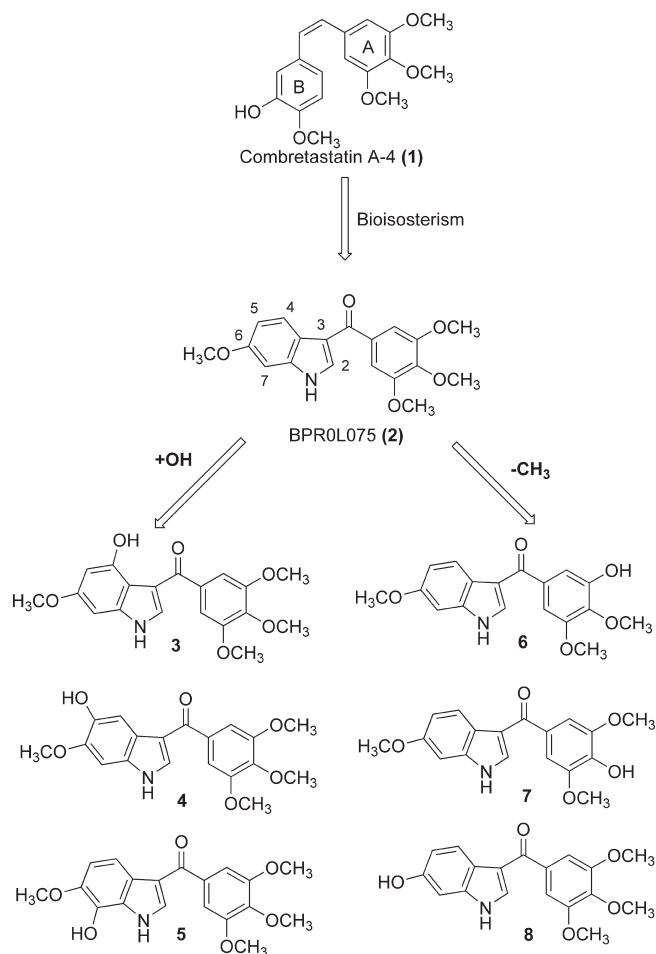
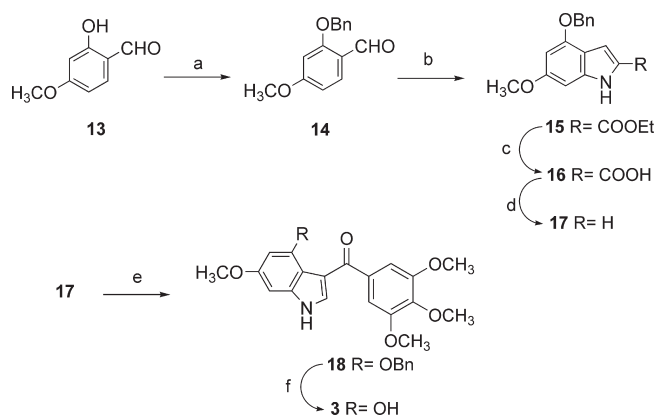


Figure 1. Structure of **2** and possible *O*-demethylated and hydroxylated metabolites of **2**.

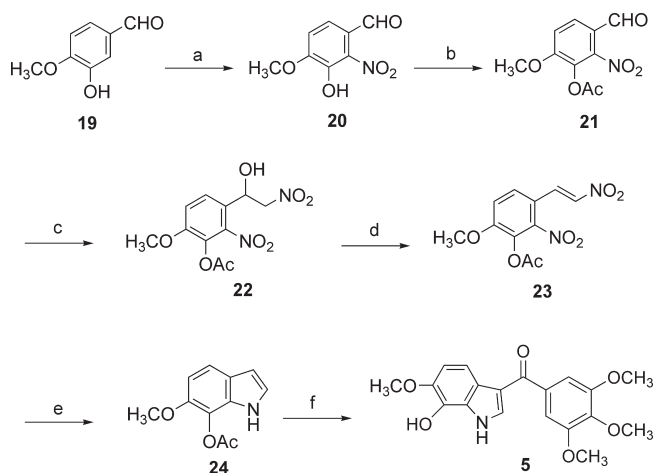
Scheme 1^a



^a Reagents and conditions: (a) BnBr, K₂CO₃, EtOH, reflux, 86%. (b) (i) N₃CH₂CO₂Et, NaOEt, EtOH, -15 °C; (ii) xylene, reflux, 74%. (c) KOH, EtOH, reflux, quantitative. (d) Copper chromite, quinoline, 215 °C, 73%. (e) ZnCl₂, EtMgBr, AlCl₃, 3,4,5-trimethoxybenzoyl chloride, CH₂Cl₂, 26%. (f) H₂, Pd/C, ethyl acetate, 89%.

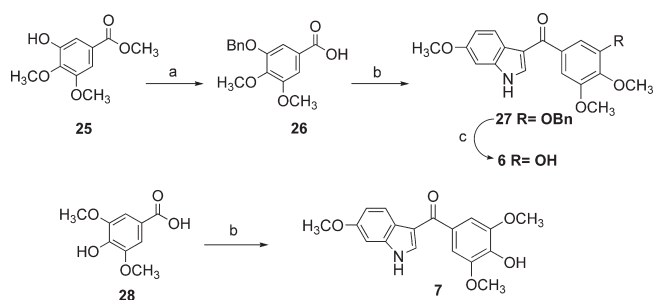
synthesis of 5-hydroxy-6-methoxy-3-(3',4',5'-trimethoxybenzoyl)-1*H*-indole (**4**) and 6-hydroxy-3-(3',4',5'-trimethoxybenzoyl)-1*H*-indole (**8**).^{5,6} The synthesis of hydroxylated metabolites **3** and **5** are depicted in Schemes 1 and 2. 4-Hydroxy-6-methoxy-3-(3',4',5'-trimethoxybenzoyl)-1*H*-indole (**3**) and 7-hydroxy-6-methoxy-3-(3',4',5'-trimethoxybenzoyl)-1*H*-indole (**5**) were obtained by Friedel–Crafts

Scheme 2^a



^a Reagents and conditions: (a) NO₂BF₄, CH₃NO₂, CH₂Cl₂, -40 °C, 50%. (b) NaOAc, Ac₂O, 60 °C, 82%. (c) KN(TMS)₂, CH₃NO₂, THF, -78 °C. (d) MsCl, CH₂Cl₂, 0 °C, 36% over two steps. (e) Fe, SiO₂, AcOH, toluene 90 °C, 31%. (f) ZnCl₂, EtMgBr, AlCl₃, 3,4,5-trimethoxybenzoyl chloride, CH₂Cl₂, 45%.

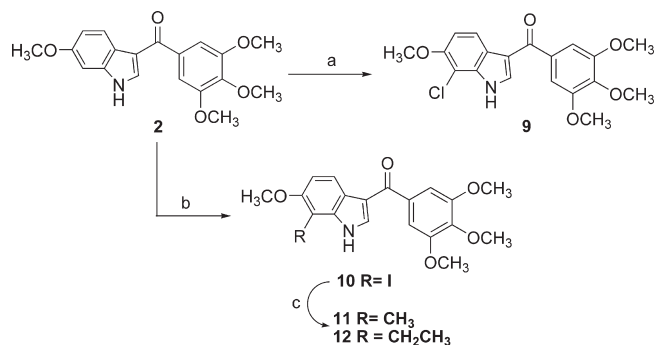
Scheme 3^a



^a Reagents and conditions: (a) (i) BnBr, K₂CO₃, EtOH, reflux; (ii) LiOH, MeOH, 88%. (b) (i) SOCl₂, CH₂Cl₂ or THF; (ii) ZnCl₂, EtMgBr, AlCl₃, 6-methoxyindole, CH₂Cl₂, 25% for **7**. (c) H₂, Pd/C, ethyl acetate, 22% over two steps for **6**.

acylation of respective indoles **17** and **24** with 3,4,5-trimethoxybenzoyl chloride. 4-Benzyloxy-6-methoxy-1*H*-indole (**17**) was synthesized in four steps from 2-hydroxy-4-methoxybenzaldehyde (**13**) as reported by Kita et al.¹⁰ Briefly, benzylation of 2-hydroxy-4-methoxybenzaldehyde (**13**) followed by Hemetsberger–Knittel indole synthesis to construct the indole core afforded **15**. Hydrolysis of ester **15** and subsequent decarboxylation under thermal conditions gave the desired indole, **17**. To construct the indole ring of 7-acetoxy-6-methoxy-1*H*-indole (**24**), the *o*,*β*-dinitrostyrene reductive cyclization method, as reported by Fukuyama et al., was applied using isovanillin (**19**) as the starting material.¹¹ Briefly, nitration of isovanillin (**19**) followed by acetylation yielded **21**. Condensation of **21** with nitromethane using KN(TMS)₂, followed by dehydration using MsCl, resulted in *o*,*β*-dinitrostyrene compound **23**. Silica gel-assisted reduction of the nitro group in **23** with Fe/AcOH, with concomitant cyclization, afforded required indole **24**.

The synthesis of demethylated metabolites **6** and **7** are shown in Scheme 3. Benzylation of 3-hydroxy-4,5-dimethoxybenzoic acid methyl ester (**25**) followed by LiOH hydrolysis in methanol produced acid **26**. Conversion of the acid to acid chloride, followed by Friedel–Crafts acylation with 6-methoxyindole, resulted in the formation of benzyl-protected **27**,

Scheme 4^a

^a Reagents and conditions: (a) NCS, AcOH, 53%; (b) NIS, AcOH, 40%; (c) Fe(acac)₃, NMP, RMgBr, THF, 0 °C → room temperature, 37% for **11** and 28% for **12**.

which was then deprotected by hydrogenation to give the desired 3'-OH metabolite **6**. For the synthesis of 4'-OH metabolite **7**, syringic acid (**28**) was treated with thionyl chloride to give the acid chloride, which was immediately converted to the desired product, **7**, through Friedel–Crafts acylation with 6-methoxyindole.

The preparation of metabolite-derived analogues **9–12** are shown in Scheme 4. 7-Chloro and 7-iodo analogues **9** and **10** were synthesized by treating parent compound **2** with NCS and NIS, respectively. 7-Iodo analogue **10** was then subsequently converted to 7-alkyl analogues **11** and **12** by iron-catalyzed cross-coupling reaction with the required Grignard reagents.

Biological Results and Discussion

Figure 1 shows all the *O*-demethylated and hydroxylated analogues of **2** that were synthesized. Compounds **2–8** were subjected to antiproliferation evaluation against KB (human cervical carcinoma), H460 (human lung cancer), and HT-29 (colorectal carcinoma) cell lines; the results are shown in Table 1. Compared to compound **2**, the *O*-demethylated metabolites **6–8** showed decreased cytotoxicity, confirming the importance of all the methoxy moieties as reported previously.¹² In contrast to the *O*-demethylated metabolites, the hydroxylated metabolite **4** displayed a loss of cytotoxicity more than 1000-fold, revealing that hydroxylation at the fifth position of **2** is not tolerated. Similarly, hydroxylation at the fourth position of the parent compound also led to loss of activity by more than 3 orders of magnitude in all three cell lines tested for compound **3**. In contrast to compound **3** and metabolite **4**, the seventh position hydroxylated metabolite **5** exhibited potent cytotoxicity in a range similar to that of the parent compound **2** for the KB cell line. Thus, out of the five metabolites synthesized for **2**, the minor metabolite **5** showed potent cytotoxicity similar to parent compound **2**, while the major metabolite **8** was at least 100-fold less active than the parent compound **2**. A similar finding, that hydroxylation at the seventh position (**5**) of the parent compound **2** is well tolerated, while the fifth position hydroxylated analogue **4** losses activity was recently reported by another group, further substantiating our results.¹³ In addition, it was found that metabolite **5** was sensitive to air/light oxidation, as reported by Ty et al.;¹³ this precluded further development of this compound, so we streamlined our efforts to identify analogues of **5**.

Hence, we began to investigate the effect of introducing different substituents at this position of indole on growth

Table 1. Cytotoxicities (IC₅₀) of Compounds **2–12** in Three Different Cell Lines

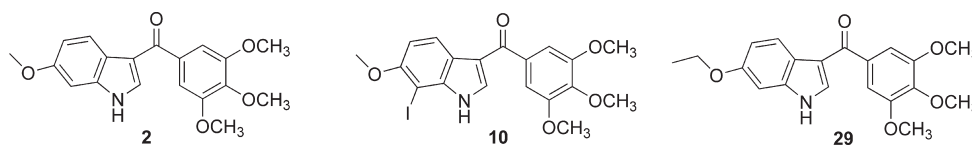
compd	IC ₅₀ (nM ± SD) ^a		
	KB	H460	HT-29
2	1.78 ± 0.52	1.0 ± 0.3	1.1 ± 0.2
3	23500 ± 4900	38000 ± 9900	45000 ± 7100
4	3100 ± 300	3100 ± 100	2700 ± 200
5	2.2 ± 1.4	29.3 ± 5.1	98.9 ± 8.6
6	48.0 ± 1.0	220.7 ± 48.5	226 ± 21.2
7	73.7 ± 12.1	189.3 ± 15.0	276 ± 25.6
8	103.0 ± 13.0	218.5 ± 12.0	100.5 ± 7.8
9	9.0 ± 1.0	9.1 ± 0.6	2.5 ± 0.1
10	0.24 ± 0.05	0.04 ± 0.01	0.35 ± 0.2
11	2.9 ± 0.6	4.1 ± 0.3	13.3 ± 7.6
12	84.3 ± 11.0	88.3 ± 5.6	75.7 ± 6.4
colchicine	11.0 ± 2.0	18.0 ± 7.0	10.0 ± 2.0

^a Values are expressed as the mean of at least three independent experiments.

inhibition against cancer cell lines. Thus, when an alkyl substituent was introduced at the seventh position of indole of parent compound **2**, the activity was retained for methyl analogue **11**, while ethyl analogue **12** had lower cytotoxicity. Introduction of chloro and iodo functions at the seventh position, however, led to potent cytotoxicity in **9** and **10**, respectively. Of particular interest is the iodo analogue **10**, which showed potency in the picomolar range (40–350 pM) for all three cell lines tested. It is noteworthy that the IC₅₀ of iodo analogue **10** was as low as 40 pM in the H460 cell line.

It is established that the growth inhibition of cancer cells by compound **2** is associated with its binding to the colchicine-binding site of tubulin.⁷ To reason for the differences in cytotoxicity of compounds **3**, **4**, and **5**, which differ at the position of the hydroxyl group, the ability of these compounds to inhibit colchicine binding to the colchicine-binding site of tubulin and their ability to inhibit tubulin polymerization was determined; the results are shown in Table 1s of Supporting Information. Among the three compounds, **5**, which has potent cytotoxicity, demonstrated higher binding affinity toward the colchicine-binding site of tubulin as it replaced >95% of [³H] colchicine at concentrations as low as 1 μM and also inhibited tubulin polymerization in vitro. Additionally, compound **10**, the iodo analogue of **5**, showed potent inhibition of tubulin polymerization and colchicine site binding; compounds **3**, **4**, and **12**, which have lower cytotoxicity, showed less binding affinity toward the colchicine-binding site and had poor ability to inhibit tubulin polymerization. These results suggest that the greater ability of compounds **5** and **10** to bind to the colchicine-binding site and inhibit tubulin polymerization leads to potent cytotoxicity for these analogues.

As the colchicine binding results for compounds **3–5** have shown good correlation between cytotoxicity and the compounds' ability to inhibit the colchicine binding, we undertook molecular modeling studies to investigate probable reasons for the different levels of binding of the compounds **3–5** to the colchicine-binding site of tubulin. This could help reveal the role of the position of hydroxyl groups in determining the binding efficacy to the colchicine-binding site. The most probable orientation of **1–5** in the colchicine-binding site (PDB ID: 1SA0) was determined by molecular docking using Gold (Figure 1s of Supporting Information). The docking of compound **2** coincides very well with **1**, and a hydrogen bond was observed between the 3-OH group of **1** and the backbone NH of Val-181 residue. The docking results of compounds **3** and **4** revealed that the 4- or 5-hydroxyl group hindered the

Table 2. Comparative in Vitro and in Vivo Profile of **2**, **10**, and **29**

compd	KB IC ₅₀ ^a (nM)	colchicine binding ^{a,b}	tubulin polymerization IC ₅₀ (μ M) ^a	in vitro metabolic rate ^a (pmol/min/mg protein)				in vivo pharmacokinetics ^a		
				mouse	rat	dog	human	CL	AUC	<i>t</i> _{1/2}
2	1.78 ± 0.52	98.2 ± 2.9	3.3 ± 0.5	71.0 ± 1.9	57.4 ± 5.6	38.0 ± 10.2	43.5 ± 4.4	29.8 ± 9.1	2739 ± 760	5.8 ± 1.7
10	0.24 ± 0.05	96.04 ± 0.12	3.5 ± 0.4	56.3 ± 0.9	39.3 ± 8.5	28.3 ± 9.7	25.1 ± 11.3			
29	1.92 ± 0.68	104.4 ± 4.8	2.2 ± 0.7	66.0 ± 5.4	46.8 ± 7.6	36.8 ± 3.0	20.0 ± 6.2	21.6 ± 4.4	4585 ± 803	11.5 ± 3.1

^a Values are expressed as the mean of at least three independent experiments. ^b Percentage inhibition of [³H] colchicine binding; [³H] colchicine and test compound concentration was at 5 μ M.

compounds from binding in the same orientation as that of **1** due to steric clash with Met-259, which resulted in binding of these compounds in a different orientation than that of **1**. In contrast, the hydroxyl group from the seventh position of indole moiety appeared to pose less steric hindrance to the binding of **5** in an orientation similar to that of **1**. Moreover the seventh-position OH group is within hydrogen-bonding distance of the backbone NH of Val-181, which could be the reason for the potent colchicine binding affinity and cytotoxicity of **5**.

Through the synthesis of metabolites **4–8** and the testing of them for cytotoxicity, we found that the *O*-demethylation of parent compound **2** at the sixth position of indole led to the formation of major metabolite **8** in vitro. The major metabolite **8** is at least 100-fold less potent in cytotoxicity assay than parent compound **2**. In addition, metabolite **8** failed to show antitumor activity in the human KB tumor xenograft animal model at 50 mg/kg (data not shown), while parent compound **2** was active at 50 mg/kg.⁷ On the basis of these findings, we reasoned that blocking the major inactivating *O*-demethylating metabolic route through appropriate structural modification of **2** could improve the in vivo exposure time of the active compound and hence improve the therapeutic efficacy. To realize this goal, we selected 6-ethoxy analogue **29**, which was previously synthesized and showed similar levels of in vitro cytotoxicity in a variety of cancer cell lines as that of 6-methoxy analogue **2**.⁵ We also observed that both compounds **2** and **29** possessed similar levels of KB cell line cytotoxicity and colchicine binding (Table 2). To investigate the possibility that the presence of bulky ethoxy group instead of methoxy group at the sixth position of indole could result in lower *O*-dealkylation reaction rate due to more steric hindrance offered by the ethyl group than the methyl group, the in vitro metabolic stability for compounds **2** and **29**, using liver microsome preparation from mouse, rat, dog, and human, were determined by measuring the amount of compound remaining unchanged after 30 min of incubation with the microsome; the results are shown as metabolic rate in Table 2. In all four species tested, the in vitro metabolic rates for **2** were higher than for **29**; the difference is particularly prominent with human enzyme, indicating that compound **29** might have slower metabolic clearance and hence higher residence time than **2** in vivo.

In addition, we have also carried out the in vitro metabolic stability of the most potent analogue identified in this study, the iodo analogue **10** (Table 2). It was found that introduction

of iodo group next to the 7-methoxy group in the indole ring had improved the metabolic stability of **10** in all the species tested. This could be due to the steric hindrance offered by the bulky iodo group next to the 7-methoxy group. Because the iodo analogue **10**, compared to **29**, has poor drug like properties, such as higher molecular weight and higher clogP, we selected **29** for further development.

On the basis of the in vitro metabolic study, to confirm if **29** indeed can have better exposure than **2**, we carried out in vivo pharmacokinetic evaluation of compound **29** and compared the data to that for **2**. Rats were dosed iv at 5 mg/kg and the PK parameters measured; the results are shown in Table 2. Compared to 6-methoxy compound **2**, 6-ethoxy compound **29** exhibited lower clearance, higher AUC, and longer *t*_{1/2}. This indicates that the in vivo “drug-elimination time” for 6-ethoxy analogue **29** is longer than for parent compound **2** and has higher drug exposure.

On the basis of the positive findings in in vivo PK studies, we set out to evaluate the in vivo antitumor activity of both

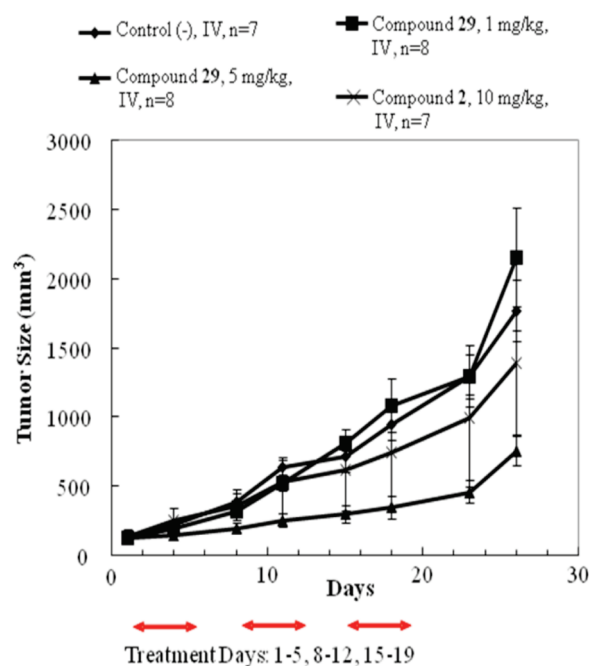


Figure 2. Inhibition of human KB xenografts' growth in vivo in nude mice by compounds **2** and **29**. Compound **29** at 5 mg/kg showed significant ($p < 0.05$) tumor growth inhibition.

compounds **2** and **29** in the KB tumor xenograft nude mouse model. Compound **2** was dosed at 10 mg/kg, and compound **29** at 1 and 5 mg/kg for five days per week for three consecutive weeks. At the dose of 1 mg/kg of compound **29**, the tumor progressed at the same rate as the untreated mice, indicating that compound **29** is inactive at this dosage (Figure 2). When the mice were treated with 5 mg/kg of **29**, KB tumor size reduced (43%) significantly ($p < 0.05$). Significant reduction in KB tumor size, however, was not observed in the mice treated with 10 mg/kg of compound **2**, showing **29** to be effective even at half of the dose. However, it should be noted that compound **29** may also be more toxic than **2**, as indicated by the percentage body weight gain after drug treatment. Compound **29** at 5 mg/kg showed body weight loss of ~5%, while **2** at 10 mg/kg showed body weight gain ~10%. Considering the fact that the in vitro cytotoxicities of compounds **2** and **29** are similar in the KB and other cell lines, compound **29** has better in vivo antitumor efficacy than **2** because of the improved PK profiles of **29**.

Conclusions

We have successfully synthesized and evaluated hydroxylated and *O*-demethylated phase I metabolites of potent antitumor agent **2**. Four of five metabolites **5**–**8** were found active against various cancer cell lines in the nanomolar concentration range. The iodo derivative **10** of the most potent 7-hydroxy metabolite **5**, exhibited extremely potent anticancer activity against cancer cell lines, with the IC₅₀ reaching picomolar potency in the KB, H460, and HT-29 cell lines. Further structure–activity relationship studies at the seventh positions of the indole may provide new insights into combretastatin analogue design in the future.

As the major *O*-demethylated metabolite **8** was at least 100-fold less active than parent compound **2**, a strategy to block the metabolic inactivation was worked out by identifying compound **29** with 6-ethoxy substituent, which could offer increased steric hindrance to *O*-demethylating metabolic deactivation reaction. Evaluation of in vitro metabolic stability and in vivo PK studies clearly demonstrated the superiority of **29** over parent compound **2** in terms of decreased in vitro metabolic rate and improved drug exposure in vivo. Further in vivo studies in the KB xenograft model showed that the antitumor effect of **29** is better than that of the parent compound **2**, validating our metabolite approach to develop potent anticancer compounds as backup candidates for novel antimitotic agent **2**. Thus, insights obtained from the synthesis and testing of in vitro metabolites of **2** were used successfully to design and develop better anticancer agents.

Experimental Section

(7-Iodo-6-methoxy-1*H*-indol-3-yl)-(3,4,5-trimethoxyphenyl)methanone (10). To a solution of NIS (0.05 g, 0.22 mmol) in acetic acid (1 mL), a solution of (6-methoxy-1*H*-indol-3-yl)-(3,4,5-trimethoxyphenyl)methanone⁵ (**2**) (0.07 g, 0.20 mmol) in acetic acid (5 mL) was added at room temperature. After the mixture was stirred at room temperature for 16 h, the solvent was evaporated under reduced pressure; the residue was purified by flash column chromatography over silica gel (EtOAc: *n*-hexane = 1:2) to give **10** (37 mg, 40%). ¹H NMR (300 MHz, CDCl₃) δ 3.89 (s, 6H), 3.94 (s, 3H), 3.99 (s, 3H), 6.95 (d, $J = 8.7$ Hz, 1H), 7.11 (s, 2H), 7.69 (d, $J = 3.0$ Hz, 1H), 8.27 (d, $J = 8.7$ Hz, 1H), 8.70 (s, br, 1H). LCMS (M + H)⁺ 468.0.

Acknowledgment. The study was financially supported by the National Health Research Institutes and National Science Council (grant no. NSC-95-2113-M-400-001-MY3), Taiwan, ROC. We thank Mark Swofford for helping with the English editing.

Supporting Information Available: General synthetic methods, synthesis, and spectral data for **3**, **5**, **6**, **7**, **9**, **11**, and **12**, HPLC purity determinations protocol, in vitro and in vivo biological evaluation protocols, colchicine and tubulin inhibition data for **3**–**5**, **10**, **12**, molecular docking studies of **3**–**5** in the colchicine-binding site of tubulin, mice body weight data for in vivo antitumor evaluation of **2** and **29**. This material is available free of charge via the Internet at <http://pubs.acs.org>.

References

- (1) Nassar, A. E.; Kamel, A. M.; Clarimont, C. Improving the decision-making process in the structural modification of drug candidates: enhancing metabolic stability. *Drug Discovery Today* **2004**, *9*, 1020–1028.
- (2) Kola, I.; Landis, J. Can the pharmaceutical industry reduce attrition rates?. *Nat. Rev. Drug Discovery* **2004**, *3*, 711–715.
- (3) Fura, A. Role of pharmacologically active metabolites in drug discovery and development. *Drug Discovery Today* **2006**, *11*, 133–142.
- (4) Liou, J. P.; Chang, J. Y.; Chang, C. W.; Chang, C. Y.; Mahindroo, N.; Kuo, F. M.; Hsieh, H. P. Synthesis and structure–activity relationships of 3-aminobenzophenones as antimitotic agents. *J. Med. Chem.* **2004**, *47*, 2897–2905.
- (5) Liou, J. P.; Chang, Y. L.; Kuo, F. M.; Chang, C. W.; Tseng, H. Y.; Wang, C. C.; Yang, Y. N.; Chang, J. Y.; Lee, S. J.; Hsieh, H. P. Concise synthesis and structure–activity relationships of combretastatin A-4 analogues, 1-aryloindoles and 3-aryloindoles, as novel classes of potent antitubulin agents. *J. Med. Chem.* **2004**, *47*, 4247–4257.
- (6) Liou, J. P.; Mahindroo, N.; Chang, C. W.; Guo, F. M.; Lee, S. W.; Tan, U. K.; Yeh, T. K.; Kuo, C. C.; Chang, Y. W.; Lu, P. H.; Tung, Y. S.; Lin, K. T.; Chang, J. Y.; Hsieh, H. P. Structure–activity relationship studies of 3-aryloindoles as potent antimitotic agents. *ChemMedChem* **2006**, *1*, 1106–1118.
- (7) Kuo, C. C.; Hsieh, H. P.; Pan, W. Y.; Chen, C. P.; Liou, J. P.; Lee, S. J.; Chang, Y. L.; Chen, L. T.; Chen, C. T.; Chang, J. Y. BPR0L075, a novel synthetic indole compound with antimitotic activity in human cancer cells, exerts effective antitumoral activity in vivo. *Cancer Res.* **2004**, *64*, 4621–4628.
- (8) Yao, H. T.; Wu, Y. S.; Chang, Y. W.; Hsieh, H. P.; Chen, W. C.; Lan, S. J.; Chen, C. T.; Chao, Y. S.; Chang, L.; Sun, H. Y.; Yeh, T. K. Biotransformation of 6-methoxy-3-(3',4',5'-trimethoxybenzoyl)-1*H*-indole (BPR0L075), a novel antimicrotubule agent, by mouse, rat, dog, and human liver microsomes. *Drug Metab. Dispos.* **2007**, *35*, 1042–1049.
- (9) Chang, Y. W.; Chen, W. C.; Lin, K. T.; Chang, L.; Yao, H. T.; Hsieh, H. P.; Lan, S. J.; Chen, C. T.; Chao, Y. S.; Yeh, T. K. Development and validation of a liquid chromatography-tandem mass spectrometry for the determination of BPR0L075, a novel antimicrotubule agent, in rat plasma: application to a pharmacokinetic study. *J. Chromatogr., B: Anal. Technol. Biomed. Life Sci.* **2007**, *846*, 162–168.
- (10) Kita, Y.; Tohma, H.; Inagaki, M.; Hatanaka, K.; Yakura, T. Total Synthesis of Discorhabdin-C—A General Aza Spiro Dienone Formation from *O*-Silylated Phenol Derivatives Using a Hypervalent Iodine Reagent. *J. Am. Chem. Soc.* **1992**, *114*, 2175–2180.
- (11) Fukuyama, Y.; Iwatsuki, C.; Kodama, M.; Ochi, M.; Kataoka, K. Antimicrobial indolequinones from the mid-intestinal gland of the muricid gastropod *Drupella fragum*. *Tetrahedron* **1998**, *54*, 10007–10016.
- (12) Hsieh, H. P.; Liou, J. P.; Mahindroo, N. Pharmaceutical design of antimitotic agents based on combretastatins. *Curr. Pharm. Des.* **2005**, *11*, 1655–1677.
- (13) Ty, N.; Dupeyre, G.; Chabot, G. G.; Seguin, J.; Tillequin, F.; Scherman, D.; Michel, S.; Cachet, X. Synthesis and biological evaluation of new disubstituted analogues of 6-methoxy-3-(3',4',5'-trimethoxybenzoyl)-1*H*-indole (BPR0L075), as potential antivasculogenic agents. *Bioorg. Med. Chem.* **2008**, *16*, 7494–7503.